Journal of Current Research in Engineering and Science
Bi-Annual Online Journal (ISSN: 2581 - 611X)

VOLUME:8, ISSUE:2, AUGUST 2025, PAPER NUMBER:19

Cancer Detection in Lung and Colon Histopathology Images Using Transfer Learning With Class Selective Image Processing

Karthikeyan.M[1], Dr.Dharmarajan.K[2]

[1]Students and [2] Faculty

School of computing Sciences

VISTAS, Chennai, India

Karthiko561@gmail.com , dharmak07@gmail.com

Abstract: Cancer contributes significantly to high mortality rates due to its aggressive nature, vast metastatic potential, and variability (leading to resistance to chemotherapy is a significant challenge in treating malignancies, particularly in lung and colon cancers, which are among the most prevalent types worldwide, affecting both men and women. timely and precise diagnosis of these cancers can significantly enhance treatment quality and increase the lifespan rates of patients. We introduce a highly precise and computationally efficient model for the rapid and accurate diagnosis of lung and colon cancers, offering an alternative to existing cancer detection methods. In this research, an extensive dataset of lung and colon histopathology images was utilized for the training and validation process. The dataset consists of 25,000 histopathology images of lung and colon tissues, evenly distributed across five classes. A pretrained neural network (AlexNet) was fine-tuned by modifying four of its layers before training it on the dataset. Initial classification results were promising for all image classes except one, with an overall accuracy of 89%. To enhance the overall accuracy while maintaining computational efficiency, rather than applying image enhancement techniques to the entire dataset, we improved the quality of the underperforming class's images by using a contrast enhancement technique that is both straightforward and effective. The application of the proposed methodology increased the overall accuracy from 89% to 98.4% while maintaining computational efficiency.

Keywords: convolutional neural networks, transfer learning, image processing, histopathology, lung cancer and colon cancer.

I. INTRODUCTION

Globally, cancer is the second leading cause of death. In 2020, over 19 million new cancer cases and 9.95 million cancer-related deaths were reported worldwide [1]. The human body is composed of trillions of cells, which grow and multiply to form new cells according to the body's needs through a process called cell division. It is normal for cells to die and be replaced by new ones when they reach a certain age or level of damage. If this process is disrupted, damaged cells begin to proliferate, leading to the development of tumors. These tumors can be either malignant (cancerous) or benign [2]. Cancer can affect any organ in the human body, but the most commonly affected areas include the colon, lungs, liver, breasts, rectum, brain, prostate, stomach, and skin. The most common cancers causing death in both males and females are lung and colon cancers. In 2020, there were 4.14 million new cases of lung and colorectal cancer, resulting in 2.7 million deaths worldwide [3].

Behavioral factors such as a high Body Mass Index (BMI), cigarette and alcohol consumption, may contribute to the onset of cancer. Radiation and ultraviolet rays are physical carcinogens, along with

certain biological and hereditary factors [3]. Symptoms of cancer include discomfort, fatigue, nausea, chronic cough, shortness of breath, weight loss, muscle pain, bleeding, and bruising [4]. However, none of these symptoms are specific to cancer, nor are they present in every individual. Consequently, detecting cancer is challenging without comprehensive diagnostic tests such as biopsy, PET scan, CT scan, MRI scan, and ultrasound. In many cases, patients exhibit no or few signs of the disease, and by the time symptoms manifest, it is often too late.

Some individuals inherit cancer-related genes from their parents. Those with an inherited risk of cancer should undergo regular checkups. However, these screening procedures are often costly, and many individuals cannot afford them. The World Health Organization suggests that about 70 percent of cancer-related deaths occur in low- and middle-income countries [3]. These nations need to establish numerous laboratories and diagnostic facilities equipped with necessary equipment and train medical personnel to conduct diagnostic procedures. Additionally, individuals living below the poverty line should be able to afford the costs of these tests.

This issue may be addressed by a field outside of medicine and healthcare. Pathology employs Machine Learning (ML) in various ways, including disease detection and the development of intelligent systems that prescribe conventional medications based on a patient's symptoms [5]. Machine learning approaches have been employed to classify and predict various types of biomedical data. Deep learning (DL) techniques enable machines to analyze high-dimensional data such as images, multidimensional anatomical representations, and videos. As a subset of ML, DL utilizes algorithms inspired by the structure and function of the brain [6].

Accurate categorization of histopathology images is crucial in obtaining reliable diagnoses of diseases in clinical practice. This task could be automated using ML algorithms, particularly DL, to replace the laborious and costly efforts of human specialists, while also meeting the requirements for high accuracy, large datasets, and other factors. Transfer learning (TL) is employed in visual categorization to address cross-domain learning challenges by transferring useful knowledge from a given dataset to the task domain [5]. TL enables the transfer of knowledge from different but related sources to target learners, enhancing performance on target domains. This can reduce the need for a vast amount of data to train target learners. TL is becoming increasingly popular and promising within ML due to its wide range of application prospects [7]. Various TL approaches include feature representation transfer, which involves cross-domain and cross-view knowledge exchange, and classifier-based information exchange, including Support Vector Machine (SVM)-based methods, TrAdaboost, and generative models [8].

TL is commonly conducted using DL models trained for the ImageNet competition, an image classification challenge featuring a vast and demanding dataset. This study utilizes the pre-trained AlexNet architecture. To leverage the intricately learned features by AlexNet in a new image classification task, several layers of the model are adjusted while keeping the weights in the transferred layers frozen.

The remainder of this paper is organized as follows: Section 2 provides a brief overview of prior research similar to ours. Section 3 describes the dataset utilized in this study and its contents. Section 4 elaborates on the proposed research model, while Section 5 presents the experimental setup and discusses the results. Finally, the paper concludes with a summary of the findings

II. RELATED WORK

Sirinukunwattana et al. [10] proposed a spatially constrained neural network for identifying cell nuclei in histopathology images of colon cancer. They utilized a novel adjacent group predictor for cell nucleus classification, achieving a maximum accuracy of 97.1%. Despite their model's favorable results, its computational efficiency fell short, with an average runtime of 50 minutes per slide. Shein et al. [11] developed an ML architecture for lung nodule malignancy classification. They employed a pooling method to extract regions of interest from feature maps and utilized max-pooling multiple times

for feature extraction from lung nodule CT scans. Notably, their approach omitted segmentation or feature extraction methods on CT scan images, achieving an accuracy of 87.14% solely based on their ML model. Three deep structured algorithms were employed for feature extraction from lung nodule CT images in [11], including stacked denoising autoencoder (SDAE), convolutional neural network (CNN), and deep belief network (DBN), with CNN achieving the highest accuracy of 89%.

Selvanambi et al. [12] conducted lung cancer detection using recurrent neural network (RNN) with the damped least-squares (DLS) method and glowworm swarm optimization algorithm, achieving 98% accuracy. Filho et al. [13] employed image segmentation for preprocessing lung nodule CT images, achieving an accuracy of 92.6% using CNN for classification. Yuan et al. [14] presented a CNN-based model for automatic polyp detection in colonoscopy videos, achieving an accuracy of 91.4% after applying preprocessing operations such as edge detection, morphology, and intensity adjustments.

RestNet50 and SVM with Radial Basis Function (RBF) kernel were used for benign and malignant lung nodule classification in CT images in [15], achieving an accuracy of 92.8%. Masood et al. [16] proposed the DFCNet model, a deep CNN, for pulmonary nodule classification into four stages of lung cancer, achieving 84.5% accuracy.

Mo et al. [17] achieved 98.5% average accuracy in polyp detection in colonoscopy videos using faster region-based convolutional neural network (Faster R-CNN). Urban et al. [18] developed deep CNNs for polyp detection in expert-labeled colonoscopy images, achieving 96.4% accuracy. A model proposed in [19] utilized binarized weights with convolutional neural networks for colonoscopy frame classification, achieving 90.28% accuracy. In [20], Wolf heuristic features and a joint learning comprehensive neural network optimized for AdaBoost were used for normal and anomalous lung structure identification, achieving 98.42% accuracy.

Suresh and Mohan [21] proposed an eight-layer CNN architecture for lung lesion categorization in CT images, achieving 93.9% accuracy. Masud et al. [22] proposed a lightweight CNN architecture with four convolutional layers for pulmonary nodule detection, achieving 97.9% accuracy. In [23], lung cancer CT scans were preprocessed to preserve image brightness and remove noise, achieving 96.2% classification accuracy using an ensemble classifier.

Bukhari et al. [24] utilized three pre-trained CNNs for histopathology image evaluation of colonic adenocarcinoma, achieving 96.4% accuracy. Mangal et al. [25] analyzed digital pathology images of adenocarcinoma and squamous cell carcinoma, achieving 97.8% accuracy with a shallow neural network. Hatuwal and Thapa [26] employed a convolutional neural network for lung cancer histopathology image classification, achieving training and validation accuracies of 96.11% and 97.2%, respectively.*A.*

LIMITATIONS OF THE RELATED WORK

The preceding studies exhibit the following drawbacks:

* Inefficient algorithms leading to increased computational costs and time consumption [10], [11], [14].

* Utilization of multiple datasets with diverse scan settings, resulting in false-positive outcomes [16].

* Exploration of a limited number of classes or a less diverse dataset [19], [20], [24]–[26].

* Reported low accuracy rates [11], [13], [14], [19], [21].

The primary contributions of this paper are delineated below:

* While previous cancer detection studies primarily focused on a single cancer type, this study simultaneously identifies lung and colon cancer.

* Unlike some studies that preprocess all images in the dataset, our proposed Class Selective Image Processing (CSIP) technique selectively enhances images of a chosen class. This approach not only boosts model classification accuracy but also reduces time and computational costs.

* Enhanced learning of the pre-trained deep learning model through CSIP on histopathological slide images, enhancing contrast via histogram equalization.

* Presentation of cutting-edge outcomes for automated lung and colon cancer detection using histopathological slide images.

* Experimentation conducted on a comprehensive and balanced dataset comprising 25,000 histopathology images evenly distributed across five lung and colon classes. The incorporation of multiple classes and a large image set enhances the model's accuracy and reliability.

III. UTILIZED CANCER DATASET

In this research, we utilized the LC25000 dataset developed by A. Borkowski and colleagues, which was released in 2020 [27]. This dataset comprises 25,000 images depicting lung and colon tissues categorized into five classes. Lung tissue images consist of three types: adenocarcinoma, squamous cell carcinoma, and benign, while colon tissue images include adenocarcinoma and benign categories.

Initially, the LC25000 dataset contained 1,250 pathology slide images of lung and colon tissues. To augment the dataset, images were flipped and rotated under various conditions, resulting in an expansion to 25,000 images across five categories, with 5,000 images per category. The images were resized to dimensions of 768 × 768.

TABLE 1. Description of the employed dataset.

Image Type	Class ID	Class Title	Total Images
Colon Adenocarcinoma	0	Colon_aca	5000
Colon Benign	1	Colon_n	5000
Lung Adenocarcinoma	2	Lung_aca	5000
Lung Benign	3	Lung_n	5000
Lung Squamous Cell Carcinoma	4	Lung_scc	5000

prior to augmentation. To guarantee privacy and unrestricted use, these images are validated and adhere to the Health Insurance Portability and Accountability Act (HIPAA). Example images from the dataset are depicted in Figure 1. Table 1 displays the designated names and IDs for each image class in the dataset.

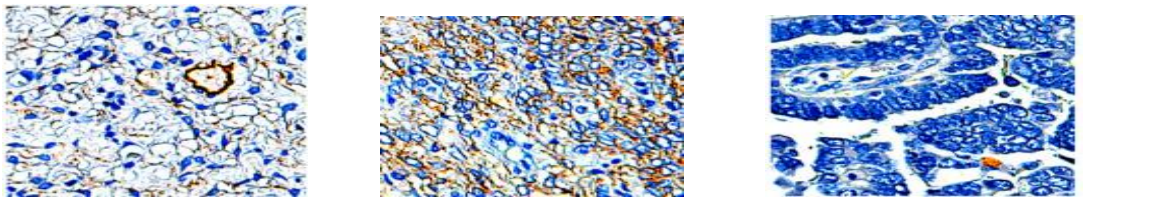

(a) (b) (c)

(d) (e)

FIGURE 1. Histopathological images from dataset. (a) Lung Adenocarcinoma. (b) Lung benig. (c) Lung squamous cell. (d) Colon Adenocarcinoma.(e) colon benign

IV. MATERIALS AND METHODS

TL, a machine learning technique, involves adapting a model designed for one task to another. DL utilizes networks pre-trained on large datasets to construct new network architectures, which can then be fine-tuned for use on new datasets. Given the time and resources required to train deep CNNs, TL significantly reduces training effort. It is often faster and simpler than building and training a network from scratch. TL is commonly executed with DL models trained for a major image classification task, such as the ImageNet competition [7].

In this study, a pretrained AlexNet model is employed for cancer image classification. AlexNet, developed in 2012 by Alex Krizhevsky, is an award-winning convolutional neural network renowned for its high accuracy on challenging datasets. This network comprises 65,000 neurons and has over 60 million parameters. The ImageNet database is an extensive collection of images, containing over 14 million images across more than 20,000 classes. AlexNet has been trained on this vast dataset

TABLE 2. Training options and parameters.

Training Options	Parameters
Image Size	227x227x3
No of Epochs	60
Initial Learning Rate	0.00001
Momentum	0.9
Solver	SGDM

The ImageNet database comprises over a million images spanning more than one thousand classes. The network architecture consists of five convolutional layers and three fully connected layers [28].For this research, the first layer and the last three layers of the model are adjusted to suit the requirements. Images were resized to 227×227×3 to comply with the model's size constraints. The dataset was divided, allocating eighty percent of the images for training and twenty percent for validation. Details of the training options and other parameters are presented in Table 2.

The proposed methodology is illustrated in Figure 2. Initially, histopathology images are obtained and resized to 227 × 227 × 3 as per the model's specifications. The resized images are then used for training and validation. The preliminary results are assessed in terms of accuracy, precision, F1-score, recall, specificity, and misclassification rate. If the results are unsatisfactory, the CSIP strategy is employed. This technique identifies the underperforming class and applies Histogram Equalization (HE) to enhance the image quality of that class. The model is then re-executed using the improved images. The proposed approach focuses on enhancing the images of underperforming classes only, rather than processing the entire dataset, which reduces processing time and effort.

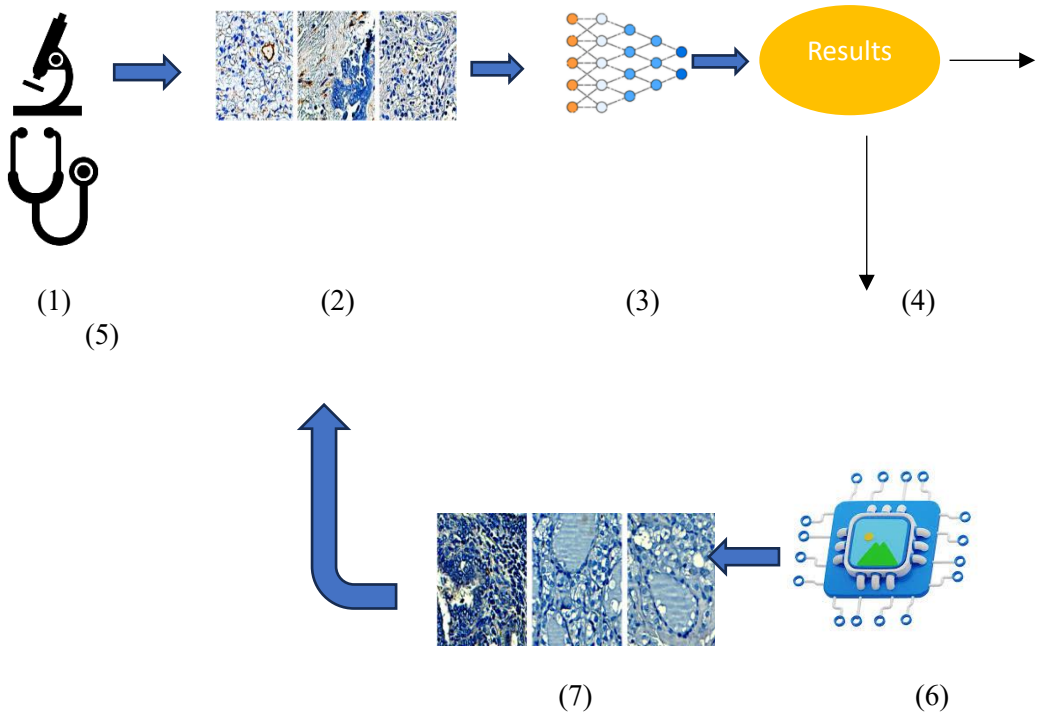

1.Acquiring Histopathology 2.Image Dataset 3.Pretrained Neural Network 4.Required Results Achieved 5. Doctor 6.Class Selective Image Processing 7.Improved Image

FIGURE 2. Proposed model for transfer learning and class selective image processing.

Image contrast enhancement stands as one of the most potent techniques for improving image quality. Among these techniques, histogram equalization emerges as particularly efficient and computationally expedient [29]. This process redistributes intensity values across an image to achieve enhanced contrast [30]. All images belonging to the underperforming class underwent histogram equalization, following which the dataset was once again utilized for training and validation.

V. RESULTS AND DISCUSSIONS

When contrasted with prior research on lung and colon cancer detection, our proposed methodology yielded encouraging outcomes. Our dataset comprises 25,000 images, evenly distributed across 5 classes. We partitioned the dataset, allocating 80% of images from each class for training the AlexNet model and reserving 20% for testing purposes. In our performance evaluation, we assessed precision, sensitivity, specificity, F1 score, recall, and misclassification rate, alongside accuracy. Below are the performance metrics employed in this investigation:

$$Specificity = \frac{}{TN + FP} \quad (1)$$

$$Precision = \frac{TP}{TP + FP} \quad (2)$$

$$F1 = \frac{TP}{TP + \frac{1}{2}(FP + FN} \quad (3)$$

$$Recall = \frac{TP}{TP + FN} \quad (4)$$

$$Accuracy = \frac{TP + TN}{TN + TP + FN + FP} \quad (5)$$

$$MisclassificationRate = 1 - (\frac{TP + TN}{}) \quad (6)$$

The training progress and confusion matrix presented in Figure 3 and Figure 4 respectively illustrate the model's performance prior to the application of CSIP. The confusion matrix not only provides the overall accuracy but also showcases the precision and recall values for each class. The model achieved an overall accuracy of 89.9%. The precision values for colon_aca, colon_n, lung_aca, lung_n, and lung_scc are 98.8%, 99.7%, 67.4%, 99.9%, and 96% respectively. Similarly, the recall values for colon_aca, colon_n, lung_aca, lung_n, and lung_scc are 99.1%, 99.9%, 97.1%, 99.8%, and 53.3% respectively.

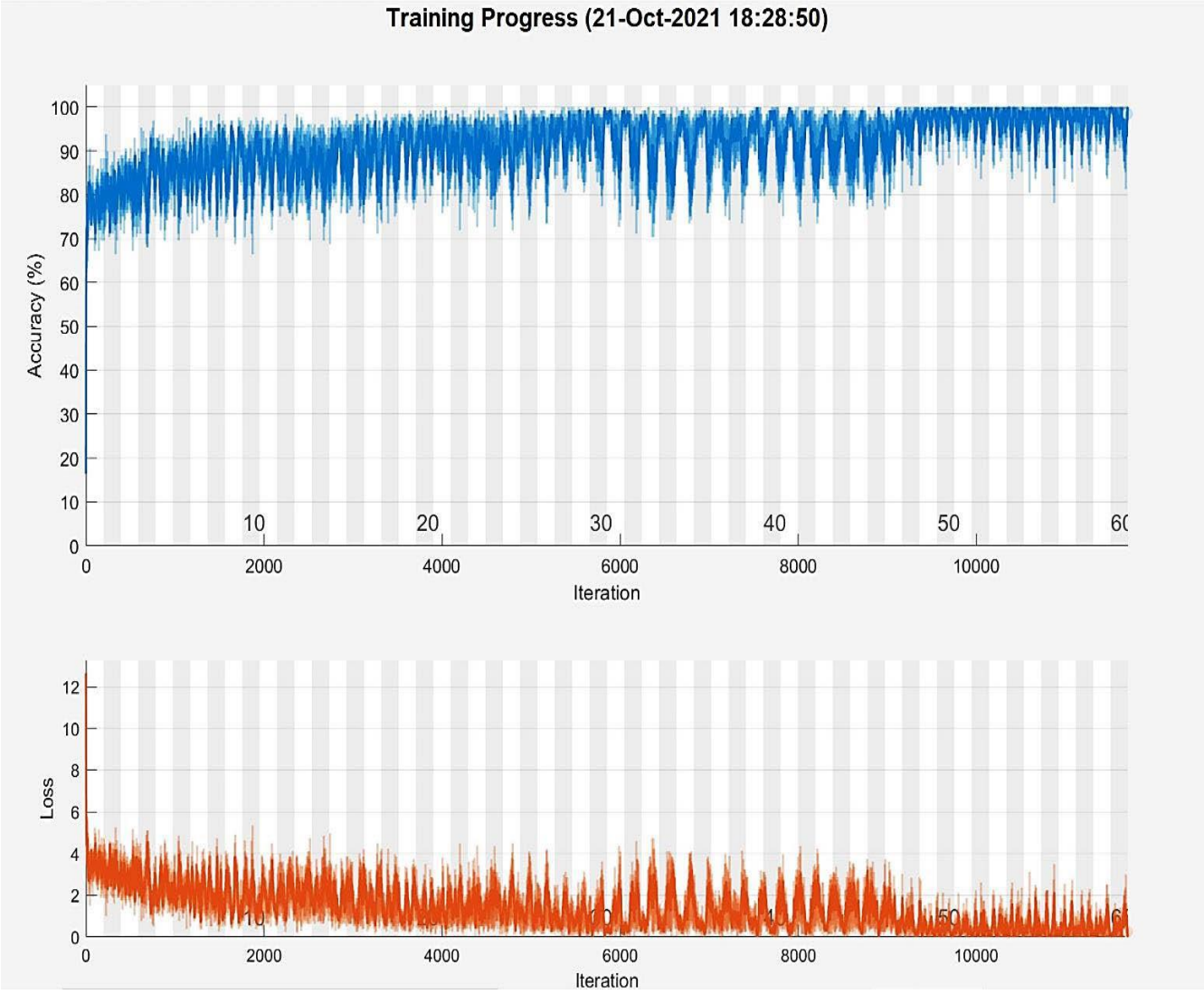

b FIGURE 3. Training progress of AlexNet before application of CSIP.

Table 3 and Figure 5 depict the model's accuracy, precision, F1 score, recall, specificity, and misclassification rate for each class in the dataset. The highest accuracy is achieved by the lung_n class, reaching 99.94%, with the lowest misclassification rate of 0.0006. The colon_n class attained an accuracy of 99.92% with a misclassification rate of 0.0008. In comparison, the colon_aca class achieved an accuracy of 99.58% with a misclassification rate of 0.0042. However, the lung_scc and lung_aca classes exhibited lower performance, with accuracies of 90.22% and 89.84% respectively, and misclassification rates of 0.978 and 0.1016.

Regarding the F1-score, the lung_n, colon_n, and colon_aca classes obtained 99.85%, 99.80%, and 98.80% respectively, while the lung_aca and lung_scc scored 79.56% and 68.55%.

To enhance the overall classification accuracy of the model, we implemented the contrast enhancement technique (HE) solely on the images of underperforming classes, thereby saving time and computational costs. The HE technique was applied to all 5000 images of the lung_scc class. Essentially, the HE technique rectifies the histogram by uniformly spreading all grey levels, resulting in a significant change in the mean brightness of the enhanced image.

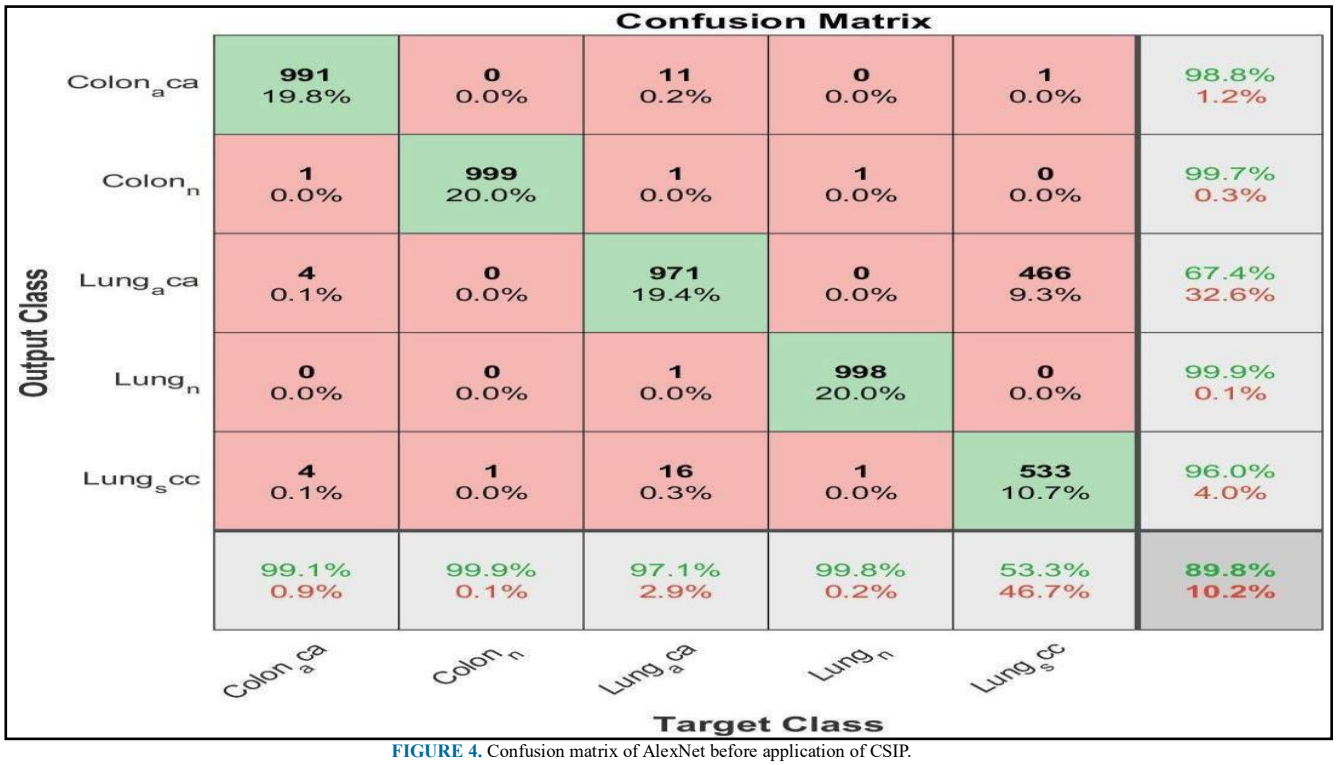

FIGURE 4. Confusion matrix of AlexNet before application of CSIP.

The relevant image is projected into the whole dynamic range

$\in [Z_0, Z_{G-1}]$, by HE using the CDF, which is denoted by the

X_k

$$C(Z) = Z_0 + (Z_{G-1}, Z_0)(\quad _{i=0} F(Z_i)(Z))$$

where n_k denotes the sum of pixels and Z_k represents the intensity level. The histogram of image S is the plot of Z_k vs. n_k while the cumulative density function (CDF) is given by [31]: only. Therefore,

images in lung_scc need to be processed for If the image has been processed using the classic, HE method, the statistical expectation E(.) of the resulting picture S is determined by:

$$E(S) = S_m = \frac{1}{2}(Z_{G-1}, Z_0)$$

where Sm represents the average intensity of the resulting image. Consequently, the image's intensity is substantially shifted towards the mean grey level. To visually demonstrate the results of the applied image processing technique, Figure 6 exhibits the original image alongside the histogram equalized image, accompanied by their respective histograms.

The confusion matrix reveals that AlexNet performed admirably on all classes of cancer images except for the lung_scc class, achieving an overall accuracy of 89.8%. The colon_aca class achieved an accuracy, precision, and F1 score of 99.58%, 98.80%, and 98.95% respectively. Similarly, the colon_n class attained an accuracy, precision, and F1 score of 99.92%, 99.70%, and 99.80% respectively. However, the lung_aca class achieved an accuracy of 90.02%, with precision and F1 score of 67.38% and 79.56% respectively. The lung_n class achieved an accuracy, precision, and F1 score of 99.94%, 99.90%, and 99.85% respectively. In contrast, the lung_scc class had an accuracy of 90.22%, precision of 96.04%, and an F1 score of 68.55%. Hence, images in the lung_scc category require quality improvement. The HE technique was applied to all 5000 images in the lung_scc class, resulting in visible contrast differences in the sample images presented in Figure 6. After optimizing the picture quality of the selected class, the dataset was updated, and the model was run for an additional 60 epochs. The adoption of CSIP resulted in a substantial increase in accuracy and other parameters in the experimental findings. Figure 7 illustrates the training progress, while Figure 8 presents the confusion matrix after CSIP. The accuracy of the Lung_scc class reached 100% after the implementation of the proposed CSIP.

TABLE 3. Performance of the model before CSIP

Type of Tissue	Accuracy	Precision	F-1 Score	Recall	Specificity	Misclassification Rate	Overall Accuracy
Colon_aca	99.58%	98.80%	98.95%	99.10%	99.70%	0.0042	**89.9%**
Colon_n	99.92%	99.70%	99.80%	99.90%	99.93%	0.0008	
Lung_aca	89.84%	67.38%	79.56%	96.14%	88.25%	0.1016	
Lung_n	99.94%	99.90%	99.85%	99.80%	99.98%	0.0006	
Lung_scc	90.22%	96.04%	68.55%	53.30%	99.45%	0.0978	

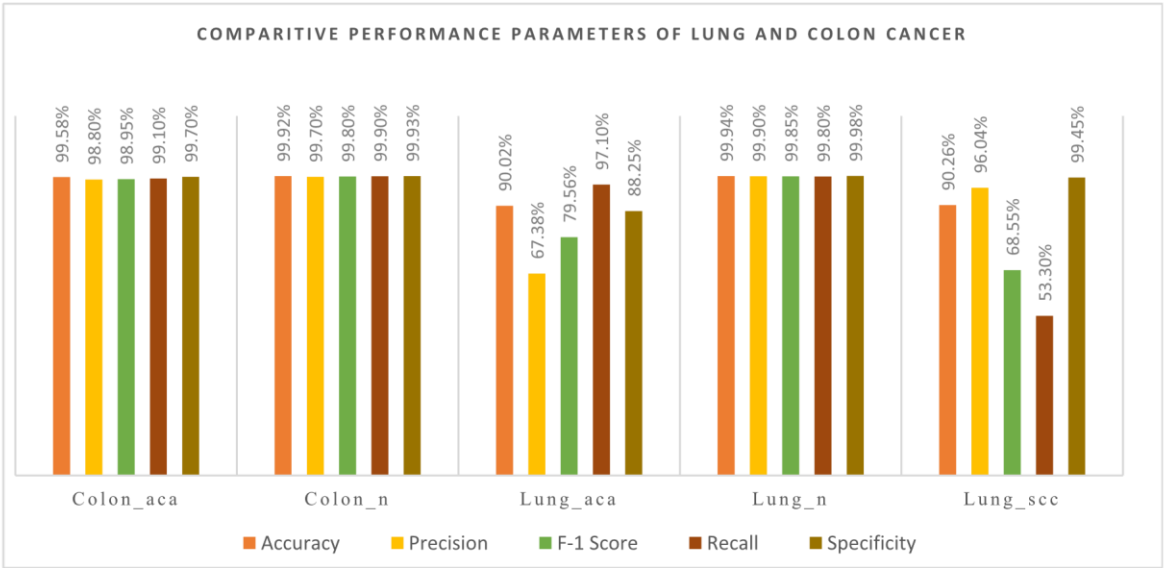

FIGURE 5. Performance of the model on each class.

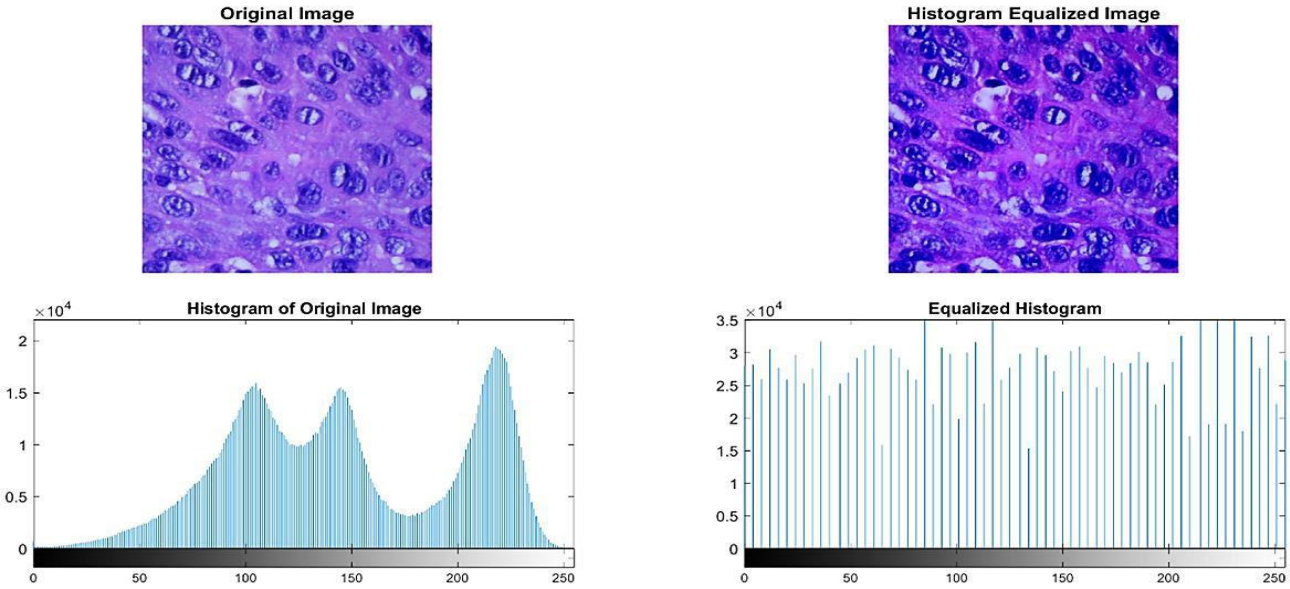

FIGURE 6. A sample image and its histogram before and after histogram equalization.

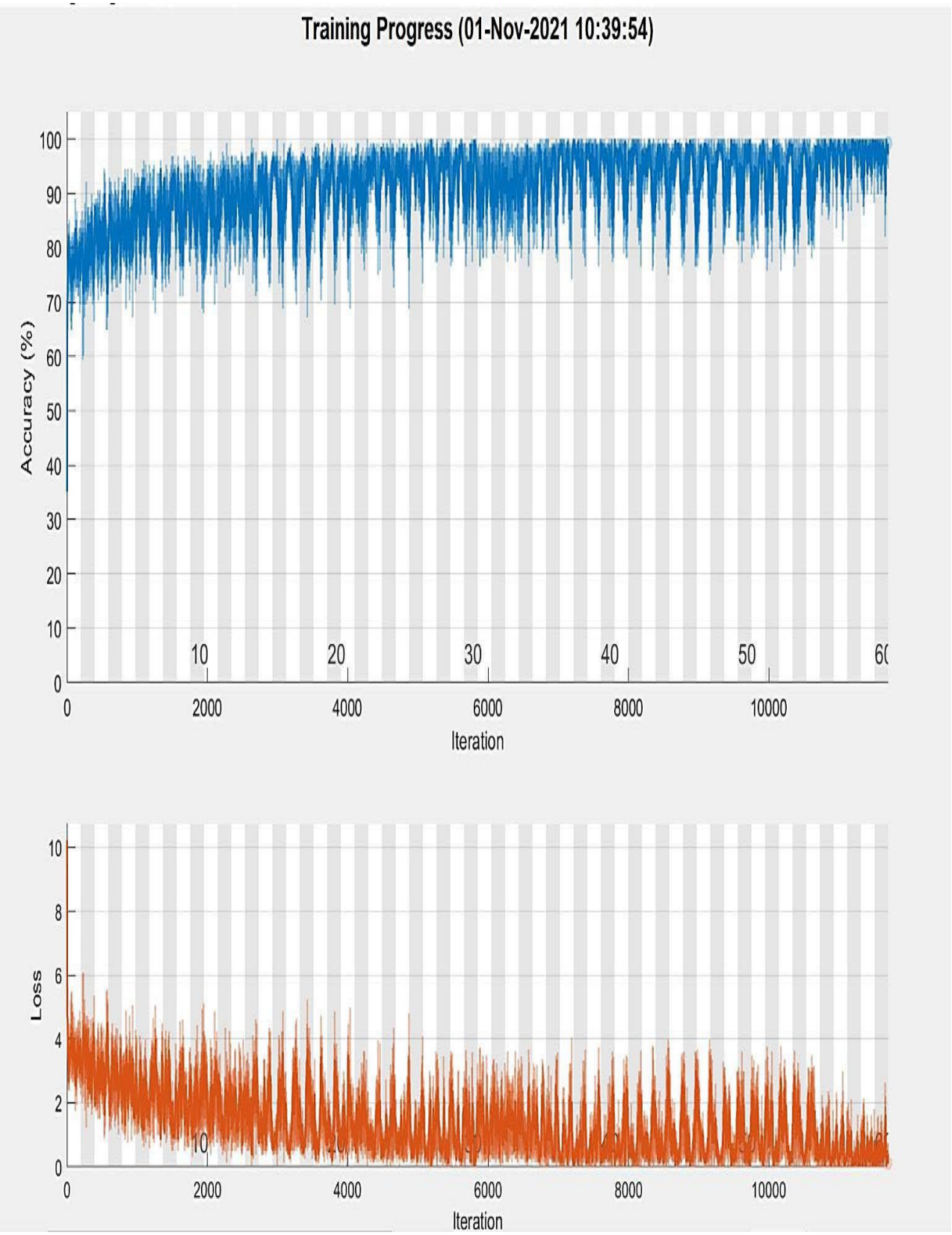

FIGURE 7. Training progress of the model after class selective image processing.

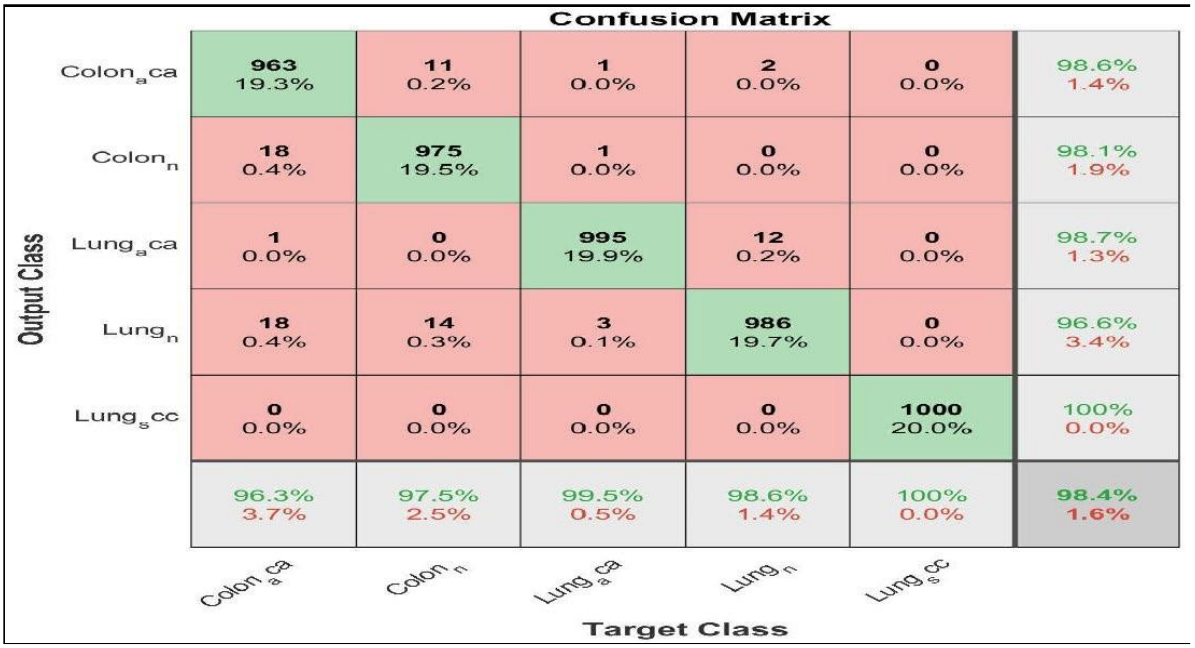

FIGURE 8. Confusion matrix of the model after class selective image processing.

TABLE 4. Post image processing results.

Type of Tissue	Accuracy	Precision	F-1 Score	Recall	Specificity	Misclassification Rate	Overall Accuracy
Colon_aca	98.98%	98.57%	97.42%	96.30%	99.65%	0.0102	**98.4%**
Colon_n	99.12%	98.09%	97.79%	97.50%	99.53%	0.0088	
Lung_aca	99.64%	98.71%	99.10%	99.50%	99.68%	0.0036	
Lung_n	99.02%	96.57%	97.58%	98.60%	99.13%	0.0098	
Lung_scc	100.00%	100.00%	100.00%	100.00%	100.00%	0	

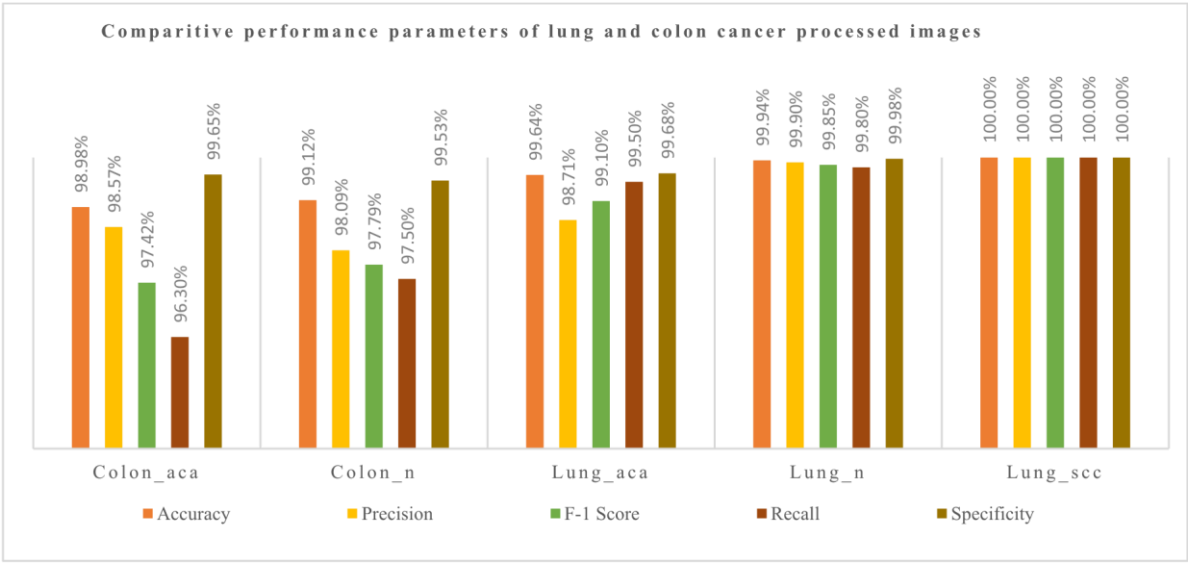

FIGURE 9. **Performance of the model on each class after CSIP application.**

The proposed model outperforms state-of-the-art methods Our approach outperforms most known methods for cancer in terms of classification accuracy when lung and colon detection, as shown in Table 6; the only exception is the anomalies are classified concurrently, as shown in Table 6. research described in [20]. The dataset utilized in [20]

TABLE 5. Overall performance of proposed CSIP-TL model.

	Training		Validation	
	Accuracy	**Misclassification Rate**	**Accuracy**	**Misclassification Rate**
Before CSIP	93.8%	0.985875	89.9%	0.040554313
Post CSIP	99.85%	0.003640	98.4%	0.00464

TABLE 6. Comparison of lung and colon cancer classification results of other methods and datasets.

Article Title	**Year**	**Type of Cancer**	**Type of Images**	**Model/Classifier**	**Accuracy (%)**
D.C. Filho et.al, [13]	2018	Lung Cancer	CT Images	Convolutional Neural Network	92.63
D. Nobrega et.al, 15	2020	Lung Cancer	CT Images	RestNet50 + SVM RBF	93.19
A. Masood et.al, 16	2018	Lung Cancer	CT Images	DFCNet	89.5
G. Urban et.al, 18	2018	Colon Cancer	Colonoscopy Frames	Convolutional Neural Network	96.4
M. Akbari et.al, [19]	2018	Colon Cancer	Colonoscopy Frames	Convolutional Neural Network	90.28
P. M. Shakeel et.al, 20	2019	Lung Cancer	CT Images	DITNN	98.42
S. Suresh et.al, 21	2020	Lung Cancer	CT Images	Convolutional Neural Network	93.9
P. M. Shakeel et. al, 23	2020	Lung Cancer	CT Images	EM	96.2
S.U.K. Bukhari et.al, 24	2020	Colon Cancer	Histopathology Images	RESNET-50	93.91
S. Mangal et.al, 25	2020	Lung Cancer	Histopathology Images	Convolutional Neural Network	97.8 9
S. Mangal et.al, 25	2020	Colon Cancer			96.61

			Histopathology Images	Convolutional Neural Network	
B.K. Hatuwal et.al, 26	2020	Lung Cancer	Histopathology Images	Convolutional Neural Network	97.2
W. Shen et.al, 34	2017	Lung Cancer	CT Images	MC-CNN	87.14
Z. Yuan et.al, [35]	2017	Colon Cancer	Colonoscopy Frames	AlexNet	91.47
T. Babu et.al, [36]	2018	Colon Cancer	Histopathology Images	RF	85.3
M. Masud et, al, 38	2020	Lung Cancer	CT scan	Convolutional Neural Network	97.9
M. Masud et.al, [39]	2021	Lung & Colon Cancer	Histopathology Images	Convolutional Neural Network	96.33
Proposed	**2021**	**Lung & Colon Cancer**	**Histopathology Images**	**CNN with CSIP**	**98.4**

only included CT scan images of the lungs, whereas our dataset encompasses both lung and colon histopathological images, making a direct comparison infeasible. Studies referenced in [24]–[26], [39] utilized the LC25000 dataset. The study cited in reference [24] focused solely on colon samples and demonstrated lower accuracy and F-measure compared to our proposed method. Although references [25] and [26] reported relatively better accuracy, they classified either lung images or colon images, not both. Consequently, the obtained results are not directly comparable, as our study considered all classes of images within the dataset for classification. In the case of reference [39], multiclass classification was performed on the LC25000 dataset, but the reported accuracy, precision, and F1-score were lower than those of our proposed model. Based on the discussions in this section, it can be concluded that the proposed approach is effective in accurately identifying lung and colon cancer tissues.

VI. CONCLUSION

Lung and colon cancers are among the leading causes of fatality worldwide. Early and accurate diagnosis of these cancers can significantly improve therapeutic outcomes and survival rates. The goal of this study was to detect lung and colon cancer accurately and efficiently. Transfer learning is employed for this detection on a dataset of 25000 histopathology images of lung and colon tissues. Our deployed DL network's overall accuracy was initially 89. %, however, after applying the proposed CSIP approach, accuracy was significantly enhanced and reached 98.8%. The proposed methodology has not only outperformed state-ofthe-art methods for lung and colon cancer detection in terms of accuracy but has also reduced the time and computational cost. We believe that our proposed methodology can also be implicated in the effective diagnosis of other diseases.

REFERENCES

1) World Fact Sheet. *International Agency for Research on Cancer*. Accessed: Oct. 17, 2021. [Online]. Available: https://gco.iarc.fr/today/ data/factsheets/populations/900-world-fact-sheets.pdf

2) (May 5, 2021). *What is Cancer*. National Cancer Institute. Accessed: Oct. 17, 2021. [Online]. Available: https://www.cancer.gov/ about-cancer/understanding/what-is-cancer

3) (Sep. 21, 2021). *Cancer*. World Health Organization. Accessed: Oct. 18, 2021. [Online]. Available: https://www.who.int/news-room/ fact-sheets/detail/cancer

4) *Cancer Symptoms and Causes*. Mayo Clinic. Accessed: Oct. 18, 2021. [Online]. Available: https://www.mayoclinic.org/ diseases-conditions/cancer/symptoms-causes/syc-20370588

5) S. Das, S. Biswas, A. Paul, and A. Dey, ‘‘AI Doctor: An intelligent approach for medical diagnosis,’’ in *Industry Interactive Innovations in Science, Engineering and Technology*. Singapore: Springer, 2018, pp. 173–183.

6) J. Schmidhuber, ‘‘Deep learning in neural networks: An overview,’’ *Neural Netw.*, vol. 61, pp. 85–117, Jan. 2015.